Supporting Information for

Comparing subsurface seasonal deoxygenation and acidification in the Yellow Sea and northern East China Sea along the north-to-south latitude gradient

Tian-qi Xiong[a], Qin-sheng Wei[b,c], Wei-dong Zhai[a], Cheng-long Li[a], Song-yin Wang[a], Yi-xing Zhang[a], Shuo-jiang Liu[a], Si-qing Yu[a]

[a] Institute of Marine Science and Technology, Shandong University, Qingdao 266237, China

[b] First Institute of Oceanography, Ministry of Natural Resources, Qingdao 266061, China

[c] Laboratory for Marine Ecology and Environmental Science, Qingdao National Laboratory for Marine Science and Technology, Qingdao 266237, China

Corresponding author: Wei-dong Zhai (wdzhai@126.com).

Contents of this file

Table S1. Summary of Cruise Information.

Figure S1. (A) Evolution of water discharge from the Changjiang (Datong Station), and (B) monthly flask analysis data of atmospheric CO_2 mole fraction at the adjacent Tae-ahn Peninsula (TAP) site (36°44′N 126°08′E) in 2017–2018.

Figure S2. (A) Comparison between measured pH_{NBS} and calculated pH_{NBS} (from field-measured TAlk and DIC), and (B) comparison between measured TAlk and calculated TAlk (from field-measured DIC and pH_{NBS}).

Figure S3. Sea surface temperature, salinity, DO saturation (DO%), TAlk, DIC, DIC:TAlk ratio, fugacity of CO_2 (fCO_2), pH_T (in situ), and aragonite saturation state (Ω_{arag}).

Figure S4. Sea subsurface temperature, salinity, DO%, TAlk, DIC, DIC:TAlk ratio, fCO_2, pH_T (in situ), and Ω_{arag}.

Figure S5. Bottom-water temperature, salinity, DO%, TAlk, DIC, DIC:TAlk ratio, fCO_2,

pH_T (in situ), and Ω_{arag}.

Figure S6. Distributions of (A–C) surface water temperature and (D–F) bottom water temperature in warm seasons.

Figure S7. Sea surface (A–C) TAlk, (D–F) DIC, (G–I) DIC:TAlk ratio, (J–L) DO%, (M–O) pH_T (in situ) and (P–R) Ω_{arag} versus salinity.

Figure S8. Plots of Ω_{arag} versus DIC:TAlk ratio in the North Yellow Sea, South Yellow Sea and northern ECS.

Introduction

Water discharge from the Changjiang River

In the year under survey (October 2017–October 2018), the hydrology of Changjiang was characterized by a wet summer and a dry winter, as well as transitional seasons of spring and autumn (Figure S1A), which was similar to the long-term average scenario during 1963–1999 (Liu et al., 2002).

Variation in atmospheric CO_2 concentration

During our seasonal cruises conducted in 2017–2018, atmospheric CO_2 mole fraction data at Tae-ahn Peninsula (TAP) site (36°44′N 126°08′E) ranged between 406 ppm (ppm = parts of CO_2 per million dry air) in August and 421 ppm in April (averaged at 416 ppm with a standard deviation of 5 ppm, Figure S1B).

Comparison between measured and calculated carbonate system parameters

To assess data quality, we collected water samples for pH_{NBS} analyses in 140 mL brown borosilicate glass bottles and preserved with 50 μL of saturated $HgCl_2$. The pH_{NBS} samples were preserved at 25°C and measured within 6 h of sampling using REX® PHSJ-4F benchtop pH meter equipped with REX® E-301-D composite pH electrode against three standard buffers (pH = 4.01, 7.00 and 10.01 at 25°C, Thermo Fisher Scientific Inc., USA). As shown in Figure S2A, most measured pH_{NBS} data and calculated pH_{NBS} (from the field-measured TAlk and DIC) were consistent at deviation level of ±0.05 pH units. To examine possible existences of organic alkalinity in our study area, we also calculated TAlk values from field-measured DIC and pH_{NBS} data. Most measured TAlk data and calculated results were consistent with each other at a deviation level of ±20 μmol kg^{-1} (Figure S2B). This deviation level was reasonably higher than the precision of TAlk determination (±2 μmol kg^{-1}). These comparisons suggested that both measured and calculated results of carbonate system parameters were reliable in this study.

Data overview of seasonal cruises in 2017–2018

Seawater temperature, salinity, DO saturation (DO%), total alkalinity (TAlk), dissolved inorganic carbon (DIC), DIC:TAlk ratio, fugacity of carbon dioxide (fCO_2),

pH_T (in situ), and aragonite saturation state (Ω_{arag}) in the North Yellow Sea, South Yellow Sea and northern East China Sea (ECS) are shown in Figures S3–S5.

Water column temperature differences during summer and autumn

The Yellow Sea Cold Water Mass (YSCWM) with a temperature of <12 °C was identified in bottom waters of the Yellow Sea during summer and autumn (Figures S6). Compared with the Yellow Sea, the northern ECS had smaller summertime temperature differences between surface and bottom waters (Figures S6B and S6E).

Sea surface carbonate system parameters and DO saturation (DO%)

TAlk behaved largely conservatively and their depth profiles were generally homogenous (Figures S3–S5). Sea surface TAlk versus salinity in the North Yellow Sea, South Yellow Sea and northern ECS showed very similar patterns with those in bottom waters (Figures 4A–4C and S7A–S7C). DIC, however, is not a conservative parameter. During warm seasons cruises, sea surface DIC (Figures S7D–S7F) were usually lower than the bottom values (Figures 4D–4F). These low surface DIC values were associated with low surface DIC:TAlk ratio (Figures S7G–S7I) and high surface DO% (Figures S7J–S7L), showing the effect of net community production. Correspondingly, relatively high values of sea surface of pH_T and Ω_{arag} were found in warm seasons (Figures S7M–S7R). Note that undersaturated DO (40–80%) and extremely low values of pH_T (~7.7) and Ω_{arag} (~1.5) were detected in very shallow regions of the northern ECS where wind-driven collapse of water stratification occasionally occurred.

Linear relationship between seawater Ω_{arag} and DIC:TAlk ratio

In the North Yellow Sea, South Yellow Sea and northern ECS, seawater Ω_{arag} values were strongly correlated with DIC:TAlk ratio and can be expressed as a function of DIC:TAlk ratio, especially within DIC:TAlk ratio between 0.83 and 0.95 (Figure S8).

Reference

Li, C. L. 2019. A comparative study of seasonal acidification in southern nearshore and central offshore waters of the North Yellow Sea (in Chinese). Master thesis, Shandong University.

Liu, X. C., Shen, H. T., and Huang, Q. H. (2002). Concentration variation and flux estimation of dissolved inorganic nutrient from the Changjiang River into its estuary (in Chinese). *Oceanologia et Limnologia Sinica* 33(5), 332–340.

Zhai, W. D. 2018. Exploring seasonal acidification in the Yellow Sea. Sci. China Earth Sci. 61: 647–658. doi:10.1007/s11430-017-9151-4

Zhai, W. D., N. Zheng, C. Huo, Y. Xu, H. D. Zhao, Y. W. Li, K. P. Zang, J. Y. Wang, and X. M. Xu. 2014a. Subsurface pH and carbonate saturation state of aragonite on the Chinese side of the North Yellow Sea: seasonal variations and controls. Biogeosciences 11: 1103–1123. doi:10.5194/bg-11-1103-2014

Table S1. Summary of Cruise Information.

Sampling period	Region	Organizer[b]	R/V	Field-measured parameters[c]	Sampling sites
13 – 16 Oct. 2017[a]	North Yellow Sea	YSFRI	*Beidou*	*T*, *S*, DO, TAlk, DIC, pH	20
13, 18 – 27 Oct. 2017	South Yellow Sea	YSFRI	*Beidou*	*T*, *S*, DO, TAlk, DIC, pH	30
31 Oct. – 7 Nov. 2017	northern ECS	YSFRI	*Beidou*	*T*, *S*, DO, TAlk, DIC, pH	30
30 Dec. 2017 – 8 Jan. 2018[a]	North Yellow Sea	NSFC	*Dongfanghong 2*	*T*, *S*, DO, TAlk, DIC, pH	14
18 – 30 Dec. 2017	South Yellow Sea	NSFC	*Dongfanghong 2*	*T*, *S*, DO, TAlk, DIC, pH	31
19 – 20 Dec. 2017	northern ECS	NSFC	*Dongfanghong 2*	*T*, *S*, DO, TAlk, DIC, pH	6
8 – 16 Apr. 2018	North Yellow Sea	NSFC	*Dongfanghong 2*	*T*, *S*, DO, TAlk, pH	14
28 Mar. – 8 Apr. 2018	South Yellow Sea	NSFC	*Dongfanghong 2*	*T*, *S*, DO, TAlk, DIC, pH	25
1 – 2 Apr. 2018	northern ECS	NSFC	*Dongfanghong 2*	*T*, *S*, DO, TAlk, DIC, pH	9
9 – 11 May 2018	North Yellow Sea	YSFRI	*Beidou*	*T*, *S*, DO, TAlk, DIC, pH	12
12 – 19 & 29 – 30 May 2018	South Yellow Sea	YSFRI	*Beidou*	*T*, *S*, DO, TAlk, DIC, pH	32
23 – 28 May 2018	northern ECS	YSFRI	*Beidou*	*T*, *S*, DO, TAlk, DIC, pH	19
2 – 5 Aug. 2018	North Yellow Sea	NSFC	*Dongfanghong 2*	*T*, *S*, DO, TAlk, DIC	18
24 Jul. – 2 Aug. 2018	South Yellow Sea	NSFC	*Dongfanghong 2*	*T*, *S*, DO, TAlk, DIC	36
12 – 20 Jul. 2018	northern ECS	NSFC	*Kexue 3*	*T*, *S*, DO, TAlk, DIC, pH	60
24 Oct. – 4 Nov. 2018	North Yellow Sea	FIO	*Xiangyanghong 18*	*T*, *S*, DO, TAlk, DIC, pH	14
14 – 24 Oct. 2018	South Yellow Sea	FIO	*Xiangyanghong 18*	*T*, *S*, DO, TAlk, DIC, pH	26
8 – 14 Oct. 2018	northern ECS	FIO	*Xiangyanghong 18*	*T*, *S*, DO, TAlk, DIC, pH	33

[a] Some of the North Yellow Sea data collected from these cruises have been reported by Li (2019).

[b] YSFRI = the Yellow Sea Fisheries Research Institute of Chinese Academy of Fishery Sciences, NSFC = the National Natural Science Foundation of China, FIO = the First Institute of Oceanography, Ministry of Natural Resources, China.

[c] *T* = temperature; *S* = salinity; DO = dissolved oxygen; TAlk = total alkalinity; DIC = dissolved inorganic carbon.

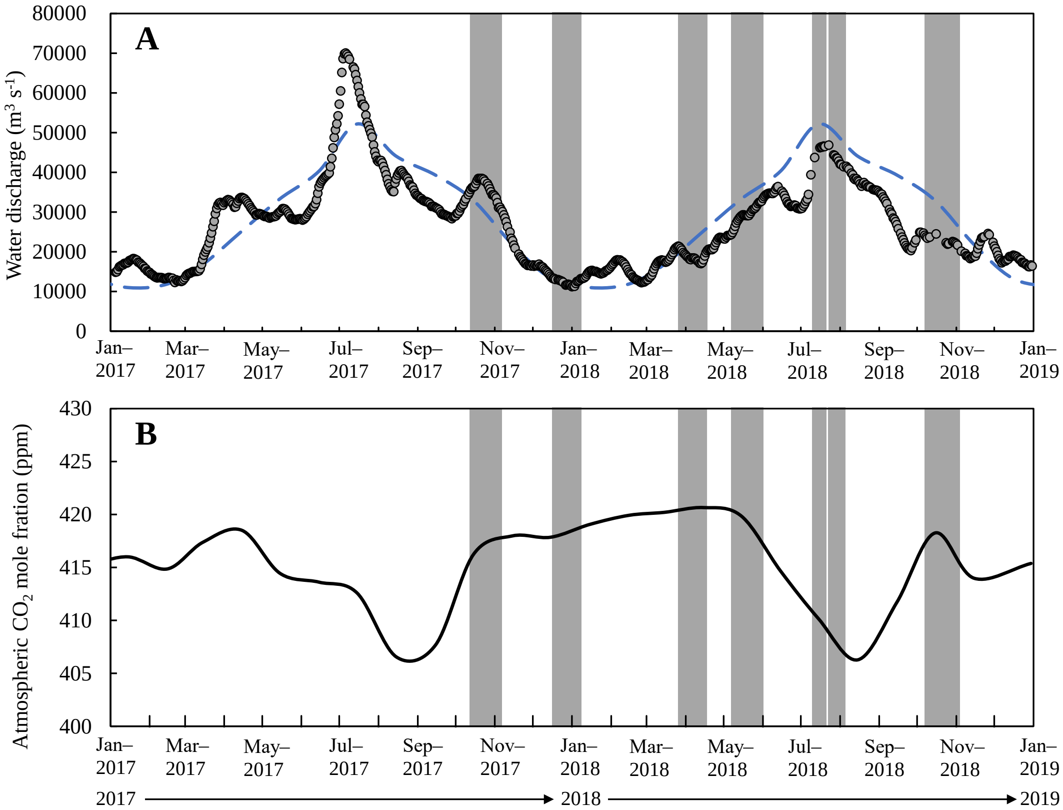

Figure S1. (A) Evolution of water discharge from the Changjiang (Datong Station), and (B) monthly flask analysis data of atmospheric CO_2 mole fraction at the adjacent Tae-ahn Peninsula (TAP) site (36°44′N 126°08′E) in 2017–2018. Water discharge data are from China Bureau of Hydrology (http://xxfb.mwr.cn/sq_djdh.html) and/or Changjiang Water Resources Commission (http://www.cjh.com.cn/), and atmospheric CO_2 mole fraction data (ppm = parts of CO_2 per million dry air) are from NOAA/ESRL's Global Monitoring Division (http://www.esrl.noaa.gov/gmd/). Grey vertical columns show sampling periods of our seasonal mapping cruises. The blue dashed curve in panel (A) represents the long-term average of monthly water discharge during 1963–1999 (Liu et al., 2002).

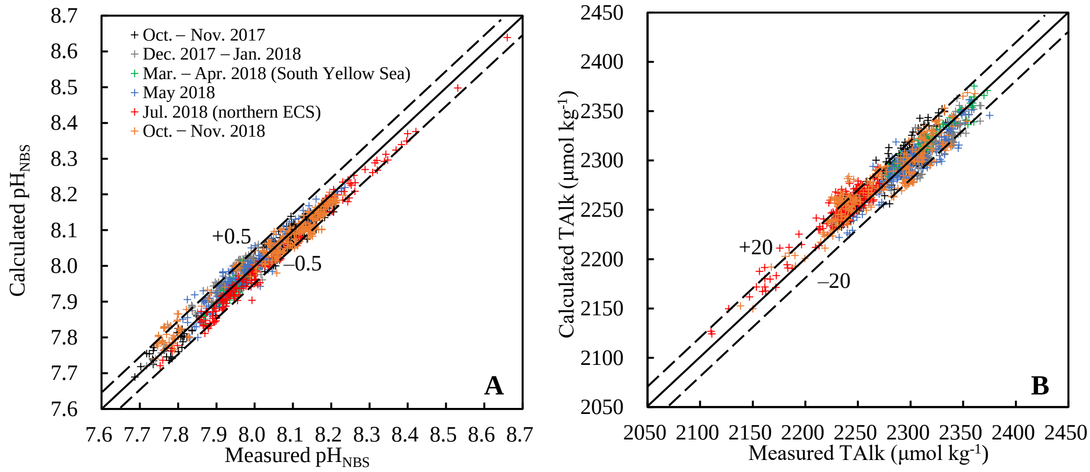

Figure S2. (A) Comparison between measured pH_{NBS} and calculated pH_{NBS} (from field-measured TAlk and DIC), and (B) comparison between measured TAlk and calculated TAlk (from field-measured DIC and pH_{NBS}). The solid line represents the 1:1 line. Dashed lines in panel (A) denote deviation level of ±0.05 units (pH_{NBS}) and dashed lines in panel (B) indicate deviation level of ±20 μmol kg^{-1} (TAlk).

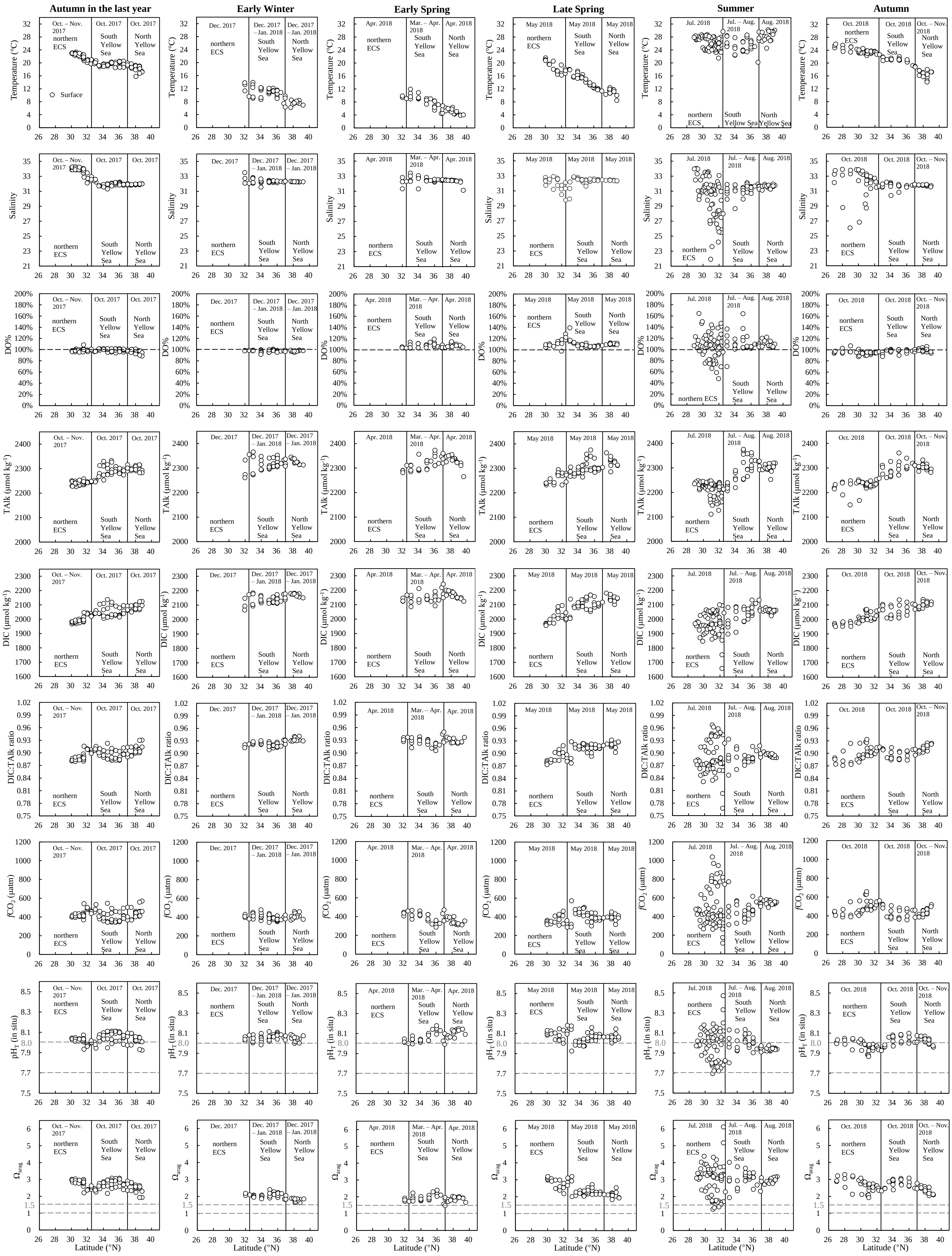

Figure S3. Sea surface temperature, salinity, DO saturation (DO%), TAlk, DIC, DIC:TAlk ratio, fugacity of CO_2 (fCO_2), pH_T (in situ), and aragonite saturation state (Ω_{arag}) in the North Yellow Sea, South Yellow Sea and northern East China Sea (ECS). Boundaries of the three coastal seas are shown as black vertical lines. The pH_T of 8.0 is comparable with the present-day air-equilibrated pH_T value, while the pH_T of 7.7 doubles the concentration of total hydrogen ions. The Ω_{arag} of 1.5 shows a critical value that the net community $CaCO_3$ dissolution occurs in the North Yellow Sea (Li, 2019; Li and Zhai, 2019), while the Ω_{arag} of 1.0 indicates the critical value for the ideal aragonite dissolution.

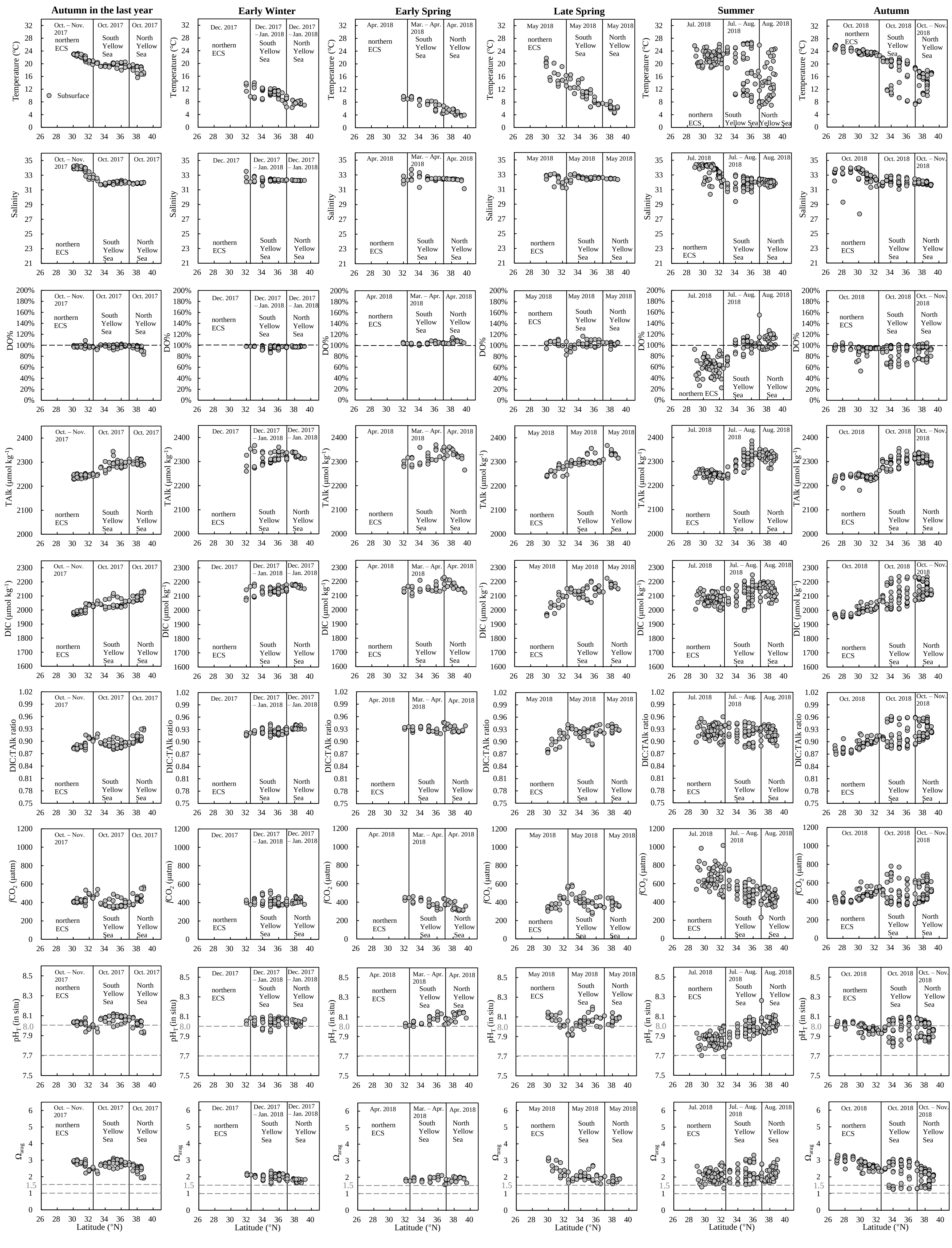

Figure S4. Sea subsurface temperature, salinity, DO saturation (DO%), TAlk, DIC, DIC:TAlk ratio, fugacity of CO_2 ($f$$CO_2$), pH_T (in situ), and aragonite saturation state (Ω_{arag}) in the North Yellow Sea, South Yellow Sea and northern East China Sea (ECS).

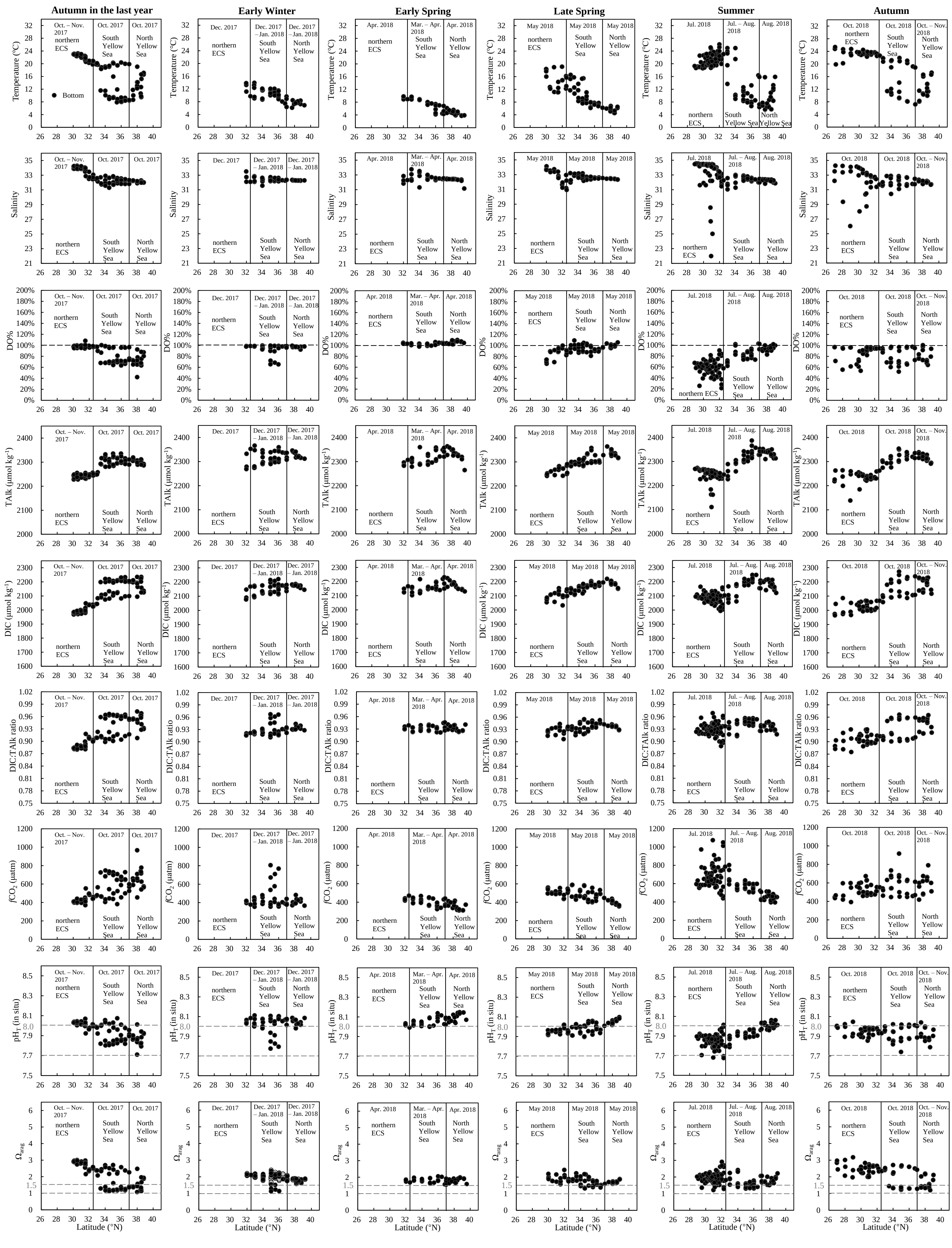

Figure S5. Bottom-water temperature, salinity, DO saturation (DO%), TAlk, DIC, DIC:TAlk ratio, fugacity of CO_2 (fCO_2), pH_T (in situ), and aragonite saturation state (Ω_{arag}) in the North Yellow Sea, South Yellow Sea and northern East China Sea (ECS).

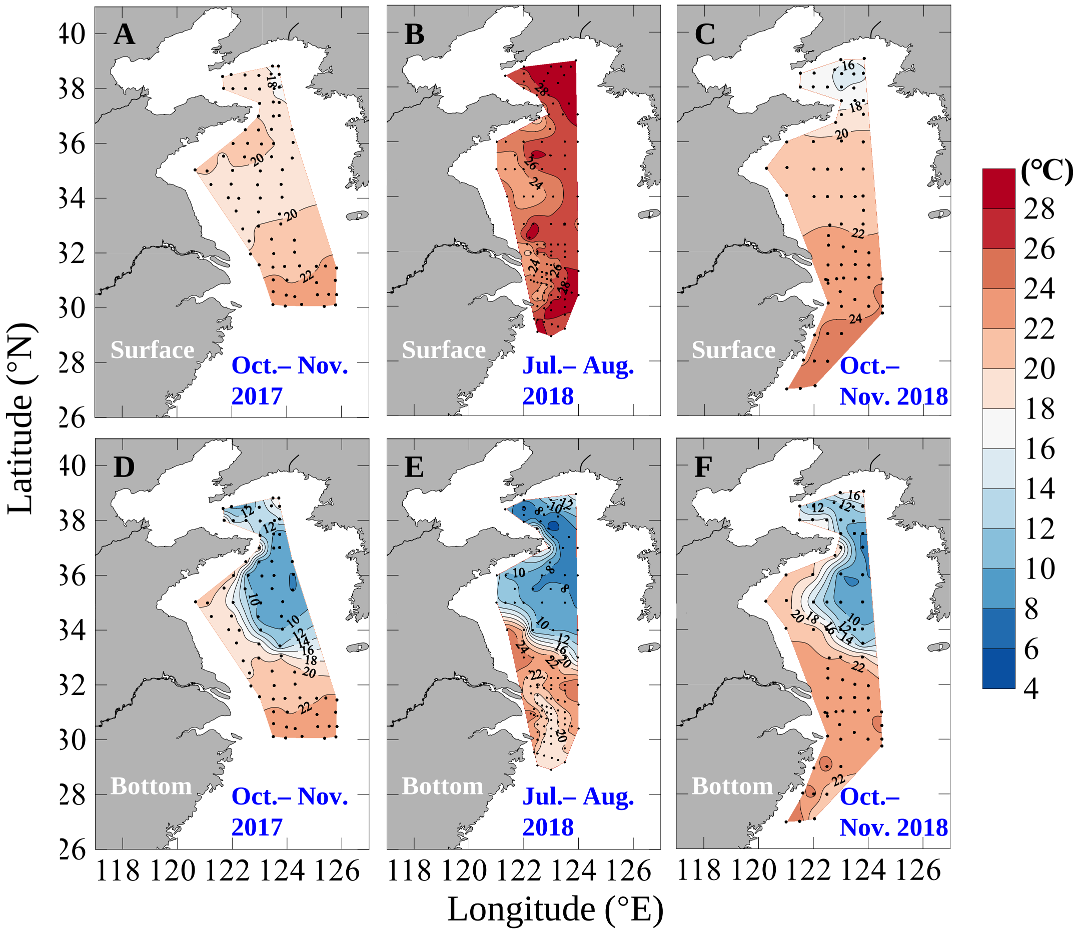

Figure S6. Distributions of (A–C) surface water temperature and (D–F) bottom water temperature during autumn 2017, summer and autumn 2018 cruises.

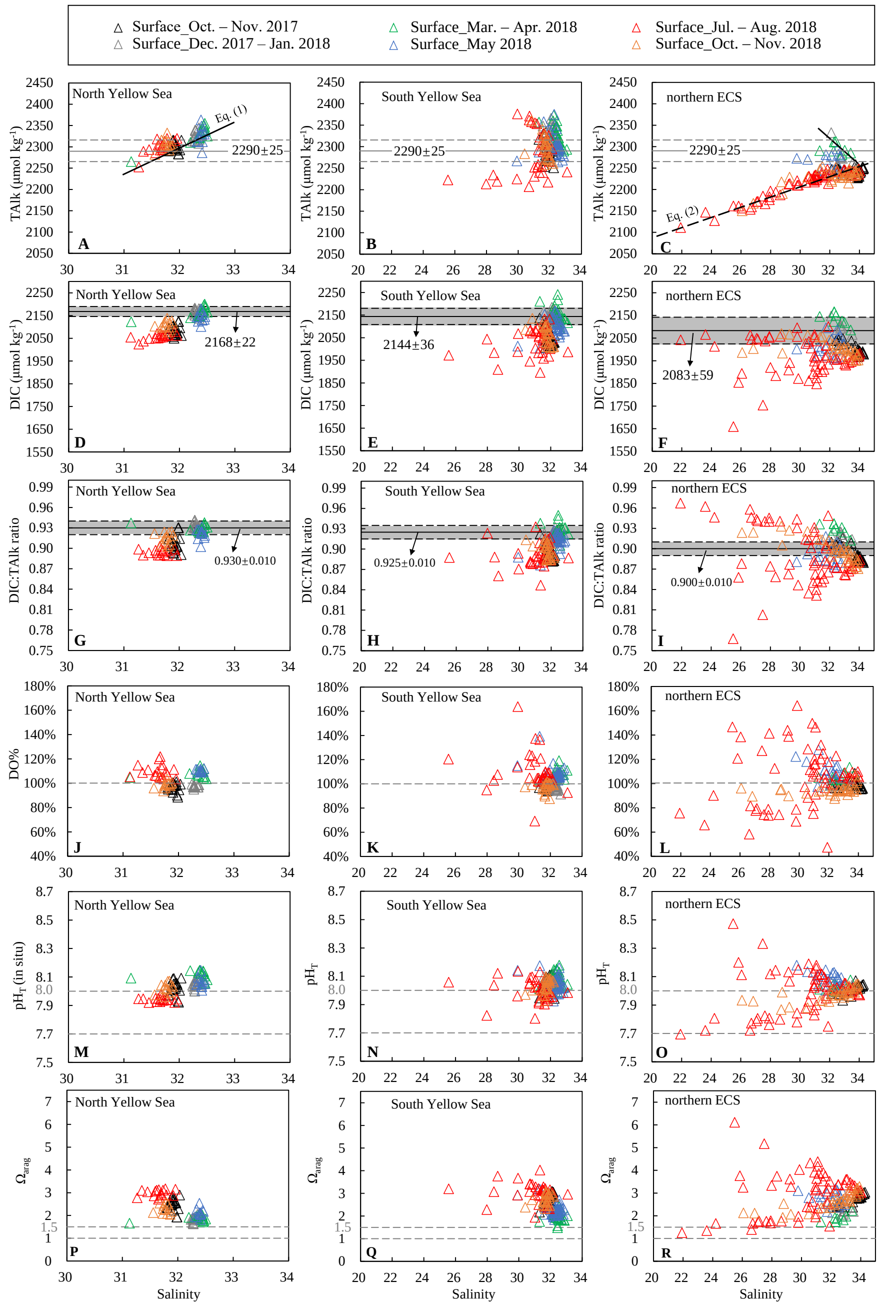

Figure S7. Sea surface (A–C) TAlk, (D–F) DIC, (G–I) DIC:TAlk ratio, (J–L) DO%, (M–O) pH_T (in situ) and (P–R) Ω_{arag} versus salinity. In panels (A)–(C), 2290±25 μmol kg^{-1} was the earlier usual value of TAlk in the Yellow Sea (Zhai et al., 2014a; Zhai, 2018). In panels (D)–(I), grey shaded areas represent mean±S.D. of wintertime/springtime DIC or DIC:TAlk ratios in individual regions. In panels (M)–(O), the pH_T of 8.0 is comparable with the present-day air-equilibrated pH_T (corresponding to a mean air-equilibrated fCO_2 value of 415±5 μatm during our seasonal cruises in 2017–2018), while the pH_T of 7.7 shows the doubled concentration of total hydrogen ions. In panels (P)–(R), the Ω_{arag} of 1.5 shows a critical value that the net community $CaCO_3$ dissolution occurs in the North Yellow Sea (Li, 2019; Li and Zhai, 2019), while the Ω_{arag} of 1.0 indicates the critical value for the ideal aragonite dissolution.

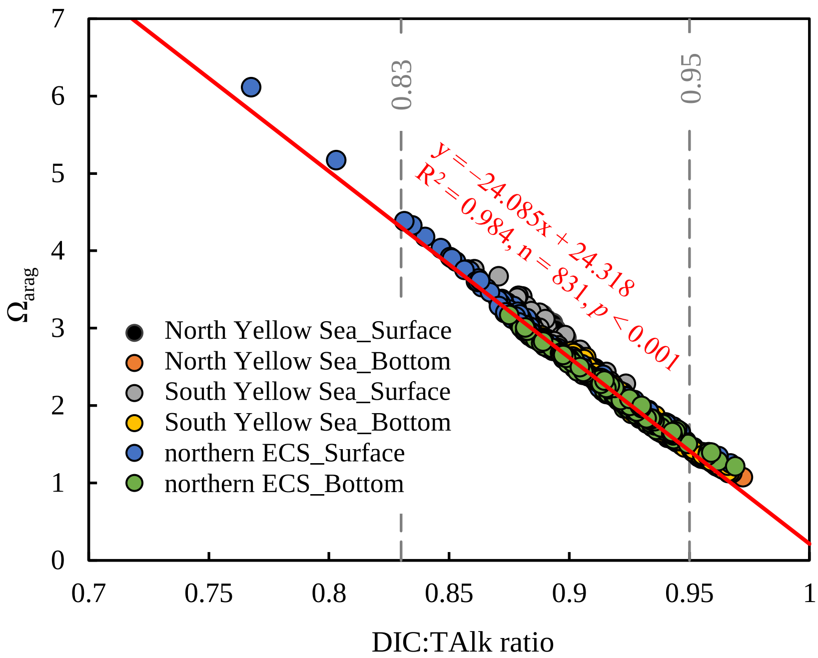

Figure S8. Plots of Ω_{arag} versus DIC:TAlk ratio in the North Yellow Sea, South Yellow Sea and northern ECS.